Accepted for publication at *IEEE Trans. Power Systems*, July 2000, paper No. PE-006PRS (08-2000).

Time Dependence of Controls to Avoid Voltage Collapse

Luis S. Vargas
Departamento Ingeniería Eléctrica
Universidad de Chile
Av. Tupper 2007, Santiago, Chile
lvargasd@cec.uchile.cl

Claudio A. Cañizares
E&CE Department
University of Waterloo
Waterloo, ON, Canada, N2L-3G1
c.canizares@ece.uwaterloo.ca

***Abstract*—In this paper, the effect of time dependence of control actions used to avoid voltage collapse, such as reactive power compensation and load shedding, is studied. A thorough justification of the phenomena under study is first presented with the help of a simple test system. The time dependence of the control actions is then studied in a real voltage collapse scenario of the Chilean Interconnected System (CIS), based on a reduced system model.**

Keywords: Power system control, voltage stability, voltage collapse, reactive power compensation, load shedding.

I. INTRODUCTION

Voltage collapse phenomena has received great attention in the power community in the last fifteen years, e.g., [1]-[3]. Moreover, the importance of voltage phenomena in determining system security and performance will continue to increase, mainly due to the continuing interconnections of bulk power systems brought about by economic and environmental pressures, which have led to increasingly more complex systems that operate closer to their stability limits [4].

In Chile, due to its longitudinal structure, the power grid is prone to experience voltage stability problems [5], [6]. In fact, there have been at least two major disturbances associated with voltage collapse in the last few years. This has attracted the attention of companies and government officials, and security procedures to avoid these types of problems are being established.

In the power systems literature, several papers have addressed the issue of time simulations to study voltage collapse phenomena [7]-[14]. In [7], the author presents an insightful study of a four-bus system using a mix of time domain and steady state analysis tools, to explain some of the basic mechanisms of voltage collapse. This work is extended in [8] to detect and identify the source of voltage instability in order to suggest remedial actions, which are then applied in [9] to a real power network, the Hydro-Quebec system. The main idea behind time simulations in these papers is that transient dynamics may be replaced by a quasi steady-state analysis using a mix of equilibrium and long term dynamic equations. In [10], a similar time simulation method is applied to a reduced test system, identifying the same basic elements as in [7] of a typical voltage collapse problem, i.e., reverse action of transformers with On Load Tap Changers (OLTC) and overexcitation limits in the generating units.

Other interesting time simulation applications in test networks as well as real systems may be found in [1], [2], and [11], together with several surveys of major incidents around the world. These surveys and simulations are mainly directed to give a detailed description of real voltage collapse events, and can be used as a basis for subsequence theoretical analyses.

In [12]-[14], systems with a longitudinal structure, similar to the Chilean system, experiencing voltage collapse incidents are presented. An incident involving oscillations and voltage decrease is reported in [12]; one of the main results arising from the corresponding fault analysis is the need for coordination of voltage controls in the system. In [13], an analysis of a voltage instability that occurred in the 400 kV Finnish network is presented. The disturbance in this case is identified as a slow voltage collapse, and the main aspects of the bus voltage evolution are reproduced using time simulations, identifying as the main cause for the collapse a shortage of reactive power in the grid. A study of voltage limitations on power systems operations is studied in [14]; the authors analyze the AEP system, deriving a set of guidelines for planning, and studying the modeling of loads and generator dynamics.

The present paper first presents a detailed theoretical discussion of voltage collapse in power systems with the help of a simple test system. The main objective of this basic analysis is to identify the main issues associated with Var compensation, load shedding and generator limits in voltage collapse phenomena considering relevant system dynamics in the time domain; a similar analysis was carried out from a static point of view in [15]. A time domain simulation technique is then used to successfully reproduce a real voltage collapse scenario that occurred on the longitudinal CIS system in May 1997 [16], presenting a diagnosis of the collapse problem. Finally, a thorough discussion of the time dependence of reactive compensation and load shedding used to avoid the collapse problems and improve transient response in the CIS system is presented. The results reported in this paper show that the effectiveness of control actions is critically dependent on the time variable, as also shown in [17].

Section II discusses the basic theoretical underpinnings of voltage collapse analysis and related tools through the study of a sample system to illustrate the main issues relevant to this paper. Section III analyzes the voltage collapse scenario of May 1997 in the CIS, pinpointing the cause that lead to the collapse problem. The time dependence of reactive compensation and load shedding to avoid voltage collapse is presented in this section as well. Finally, in Section IV, the main conclusions of this work are stated.

II. THEORETICAL ANALYSIS

The simple two-bus system of Fig. 1 is used here to illustrate the basic concepts behind the application of shunt compensation and load shedding along system trajectories in power networks. This system basically represents a generator G connected to a system S with large "inertia" trough an inductive transmission line. In this case, however, the voltage V_2 on the system side is not assumed constant, as is typically the case, but it is allowed to change so that

the system reactive power demand Q_d can be kept constant. This simple model is used to illustrate some basic issues related to system compensation and load shedding, particularly the relationship between size and "connecting" time, so that a system can be recovered after a fault that leads to collapse, and also to analyze the effect of generator Q-limits on this problem. The concepts and ideas presented on this section are later used in Section III to study an actual voltage collapse event on the Chilean interconnected system, and to devise countermeasures to avoid the collapse based on various compensation and load shedding schemes.

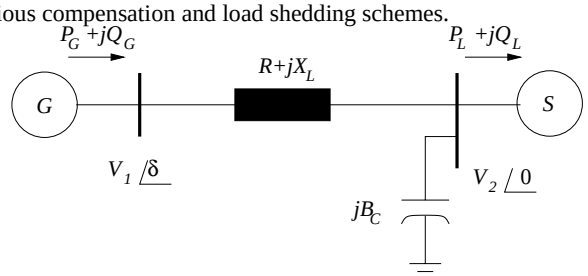

Fig. 1. Sample system.

The p.u. dynamic equations that represent this system, using a basic one-axis dynamic generator model, can be readily shown to be given by

$$\begin{aligned} \dot{\omega} &= \frac{1}{M}\left[P_m - P_G(\delta, V_1, V_2) - D_G\omega\right] \\ \dot{\delta} &= \omega \\ 0 &= P_L(\delta, V_1, V_2) - P_d \\ 0 &= Q_L(\delta, V_1, V_2) - Q_d \end{aligned} \tag{1}$$

where ω and δ and stand for the generator's angular speed and internal phasor angle and

$$\begin{aligned} P_G(\delta, V_1, V_2) &= V_1^2 G - V_1 V_2 (G\cos\delta - B\sin\delta) \\ P_L(\delta, V_1, V_2) &= -V_2^2 G + V_1 V_2 (G\cos\delta + B\sin\delta) \\ Q_G(\delta, V_1, V_2) &= V_1^2 B - V_1 V_2 (G\sin\delta + B\cos\delta) \\ Q_L(\delta, V_1, V_2) &= -V_2^2 (B - B_C) - V_1 V_2 (G\sin\delta - B\cos\delta) \end{aligned}$$

Here, Q_G is used to represent generator reactive limits; thus, if $Q_{G\min} \le Q_G \le Q_{G\max}$ the generator voltage V_1 is assumed to be controlled, i.e., kept at the fixed value $V_1 = V_{1o} = 1$, whereas if Q_G reaches a limit, V_1 is let free to change. The generator's inertia and damping constants are represented by M and D_G, respectively. The load demand is modeled through the parameter P_d and Q_d, under the assumption that that reactive power load demand is directly proportional to the active power demand, i.e., $Q_d = k\, P_d$ (constant power factor load); P_d is the main parameter that leads the test system to voltage collapse. The shunt capacitance B_C is used to illustrate the effect of compensation on the system stability; R and X_L are used to represent the generator's transmission line, transformer and internal impedance; and $G + jB = (R+jX_L)^{-1}$.

To simplify the stability analysis of this problem, the resistance is neglected ($R = 0$), i.e., $P_m = P_d$. The initial loading condition, as defined by the value of P_d, is chosen depending on whether generator limits are considered or not, as discussed below. The p.u. time constants are assumed to be $M = 1$, $D_G = 0.1$; the load power factor is assumed to be 0.97 lagging, i.e., $k = 0.25$; and the generator reactive power limits are defined as $Q_{G\max} = 0.5$ (no limits are assumed for under excitation operation, i.e., $Q_{G\max} = -\infty$). A transmission system contingency (e.g., outage of a line) is modeled by changing the value of X_L from 0.5 to 0.6. Finally, B_C is given the values of 0, 0.5, or 1 to simulate different compensation levels.

For this system, a simple Transient Energy Function (TEF) can be defined and used to *approximately* study the effect of the different system parameters, i.e., P_d, X_L and B_C, on the stability of the system; this is one of the main reason why this system was chosen to illustrate the voltage collapse problem and associated recovery strategies. Thus, as discussed in [18], [19], and [20], the stability region for system (1) can be approximately defined by

$$\begin{aligned} \vartheta(\omega, \delta, V_1, V_2) &= \frac{1}{2}M\omega^2 - B(V_1 V_2 \cos\delta - V_{1o} V_{2o} \cos\delta_o) \\ &+ \frac{1}{2}(B - B_C)\left(V_2^2 - V_{2o}^2\right) + \frac{1}{2}B\left(V_1^2 - V_{1o}^2\right) \\ &- P_d(\delta - \delta_o) + Q_d \ln\left(\frac{V_2}{V_{2o}}\right) - Q_G \ln\left(\frac{V_1}{V_{1o}}\right) \end{aligned} \tag{2}$$

where δ_o, V_{1o} and V_{2o} stand for the steady state values of the bus voltage magnitudes and angles. Observe that the generator reactive power Q_G term in this equation is not really "active" unless the generator hits a limit, in which case $V_1 \neq V_{1o}$.

Its important to stress the fact that the function defined in (2) can only be used to get a relative sense of the stability region of the test system, since is basically a Lyapunov function and hence yields only sufficient conditions for asymptotic stability [21]; furthermore, some modeling approximations were used to obtain this function, and hence it can only be considered to be an energy function [22]. For practical applications, similar energy functions are used for fast contingency screening, so that the most critical contingencies can be quickly detected and further studied in more detail through time domain simulations [23].

A. Stability Analysis

For different values of X_L and B_C, the system presents a maximum loadability point $P_{d\max}$ corresponding to the "turning" points on the PV curves of Figs. 2 and 3, for the system with and without generator limits, respectively. These maximum points are also known as the points of collapse, which in nonlinear systems theory can be shown to be either saddle-node bifurcation points for the system without generator limits (Fig. 2), or limit-induced bifurcation points for the system with generator limits (Fig. 3) [24], [25]. In these figures, the points "above" the point of collapse ("high" voltage values) correspond to stable equilibrium points (s.e.p.), whereas the points "below" ("low" voltage values) are unstable equilibrium points (u.e.p.). (This sample system cannot have Hopf bifurcations due to $R = 0$ [26], [27].)

Observe in Figs. 2 and 3 that when the contingency is applied by increasing the value of X_L, the maximum loadability point is reduced. Generator limits have a negative effect on this point as well, as these limits also reduced the maximum system loadability. On the other hand, as the compensation level increases by increasing the value of B_C, the maximum loadability point increases.

To illustrate how the stability of the system is affected by all these parameters, i.e., P_d, X_L, B_C and generator limits, the corresponding TEF profiles are obtained by evaluating (2) at the corresponding u.e.p´s. These energy profiles are depicted in Figs. 4 and 5; Fig. 4 shows the energy profile for the system without generator limits, whereas Fig. 5 illustrates the negative effect that generator limits have on this region. Observe that the area decreases as the power demand P_d increases, it increases when B_C is applied, and decreases when X_L is increased (to simulate a contingency).

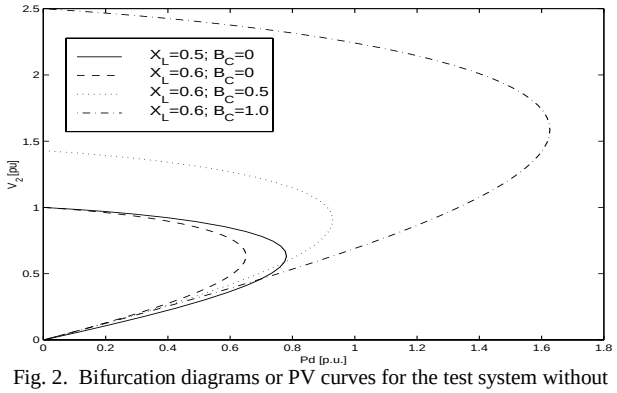

Fig. 2. Bifurcation diagrams or PV curves for the test system without generator limits. The maximum value of P_d corresponds to a saddle-node bifurcation point.

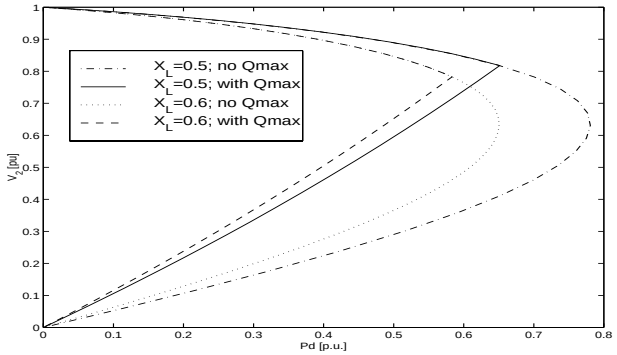

Fig.3. Effect of generator Q-limits in the bifurcation diagrams or PV curves for the test system. The maximum value of P_d corresponds to a limit-induced bifurcation point.

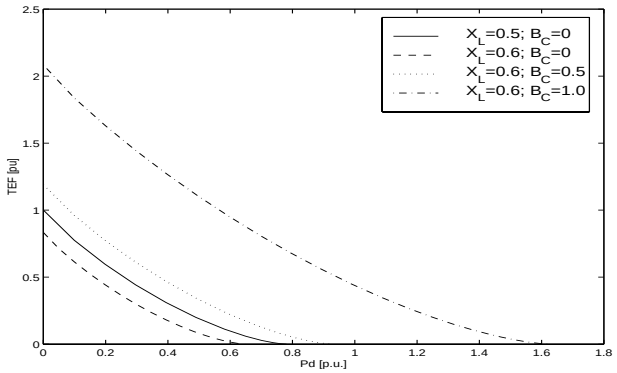

Fig. 4. TEF profiles for the test system without generator Q-limits.

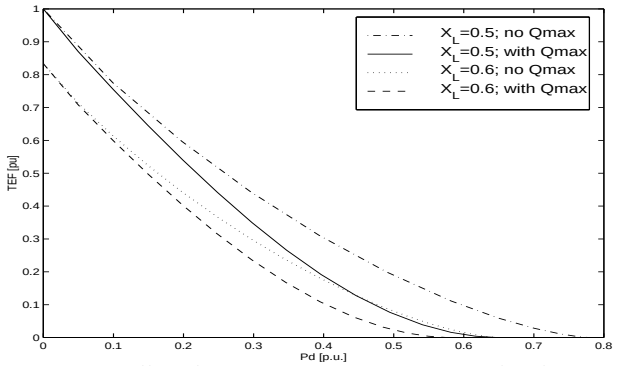

Fig. 5. Effect of generator Q-limits on the TEF profiles for the test system.

From these energy profiles, one can conclude that by applying shunt compensation or shedding load, i.e., increasing B_C or reducing P_d, respectively, the stability region of the system is increased, allowing the operator to recover the system after a fault. The question then is how fast this remedial measures should be taken to be able to recover the system, as discussed in the next section.

It is interesting to see that as B_C is increased, the stability region increases and the bifurcations move away, i.e., $P_{d\max}$ also increases. However, there is a point where this trend reverses, as explained in [18], which corresponds to a "maximum" bifurcation point; for this system, the maximum bifurcation points are obtained at $B_C = 1/X_L$. Notice also that in practice, "excessive" compensation may yield severe system overvoltages.

B. Time Domain Analysis

1) Neglecting Generator Limits: A transmission system fault at a power demand level of $P_d = 0.7$ is simulated by changing the value of X_L from 0.5 to 0.6, yielding a system collapse, as the system has no s.e.p. at the operating condition defined by $P_d = 0.7$ and $X_L = 0.6$ (see Figs. 2 and 4). The "fault" is applied at 1s, resulting in the collapse of voltage V_2 and the corresponding monotonic increase of the system frequency ω and angle δ (the fault trajectories for these variables are similar to the ones depicted in Fig. 6).

For this fault trajectory, the "potential" energies, which are obtained by subtracting the "kinetic" energy term 1/2 Mω^2 from the total TEF defined in (2), are tracked for each post-contingency equilibrium point defined by the values of X_L, B_C and P_d. The point where this energy reaches a maximum corresponds to the point where the system "leaves" the stability region; this point is known as the Potential Energy Boundary or PEB [19]. The point in time where this maximum occurs can be used as a general estimate for the "critical clearing" time, i.e., the time at which the fault should be cleared or a control action such as shunt compensation or load shedding should take place. Thus, the critical times estimates obtained using the PEB technique was 3.9 s for all recovery strategies, i.e., restore X_L to is original value of 0.5 (fault "clearance"), apply shunt compensations of $B_C = 0.5$ and $B_C = 1$, or shed load to $P_d = 0.4$.

These estimates yield just a relative idea of the actual critical times, and depending on the contingency or recovery strategy, require of full time domain simulations [23]. For the simple example discussed here, time domain simulations yield the following results: For fault clearance, the system recovers if the fault is cleared at or before 2.9 s, and does not recover if the fault is cleared at 3.0 s or longer. For a compensation level of $B_C = 0.5$ applied at or before 3.7 s, the system recovers; for connection times of 3.8 s or longer, the system does not recover. For a compensation level of $B_C = 1$, the system recovers when applied at or before 4.2 s, and does not recover if applied at 4.3 s or longer. Finally, for load shedding, the system recovers when applied at or before 3.9 s, and does not recover when applied at 4.0 s or longer. These results basically show that the "energy" analysis can be used to "adequately" estimate the connecting times in the least stressed cases, i.e., the cases where there is large compensation or load shedding; for other cases, time domain analyses are required.

2) Considering Generator Limits: In this case, a transmission system fault at a demand level of $P_d = 0.6$ is again simulated by increasing the value of X_L from 0.5 to 0.6. The system also collapses due to lack of a faulted system s.e.p. at these operating conditions, as depicted in Figs. 4 and 5. Observe that this system will not be able to operate at the previous demand level of $P_d = 0.7$.

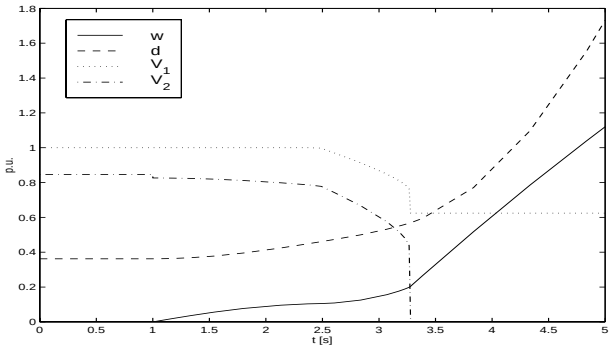

Fig. 6. System trajectories for a fault simulated by increasing X_L from 0.5 to 0.6 at 1 s when Q-limits are considered. Generator voltage control is lost at about 3 s and the system collapses.

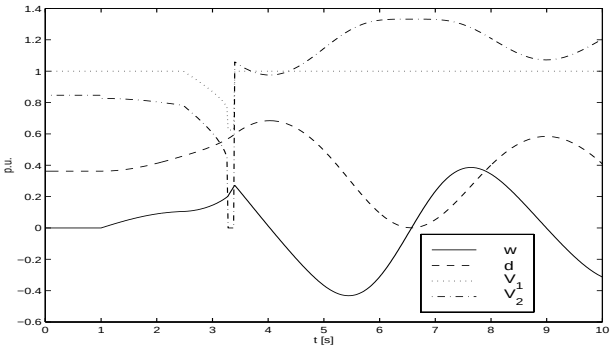

Fig. 7. System trajectories for the faulted system when considering Q-limits for shunt compensation B_C = 0.5 applied at 3.4 s. Generator voltage control is temporary lost but the system recovers.

The fault is applied at 1 s, obtaining the fault trajectory depicted in Fig. 6, which is similar to the one obtained for the system without limits. Observe that generator control of voltage V_1 is lost at about 3 s due to Q-limits, the voltage V_2 collapses and frequency ω and angle δ monotonically increase.

Once more, the "potential" energy defined with respect to a given s.e.p., which depends on the values of X_L, B_C and P_d, can be used to generally estimate the critical time for different recovery strategies, i.e., fault clearance (X_L recovery), application of shunt compensation (increase B_C), and load shedding (reduce P_d). Thus, the critical times are estimated to be 2.5 s to clear the fault, 3.3 s for compensation levels B_C = 0.5 and B_C = 1, and 3.3 s for load shedding to P_d = 0.4.

Time domain analysis yields the following results: The system recovers if the fault is cleared by changing the value of X_L back to 0.5 at or before 1.7 s, and does not recover if it is changed at 1.8 or after. If shunt compensation B_C = 0.5 is applied at or before 3.4 s, the system recovers (see Fig. 7), and does not recover for application times of 3.5 s or longer. For a compensation level of B_C = 1, the system recovers if applied at or before 3.9 s; does not recover if applied at 4 s or longer. Finally, for load shedding of P_d = 0.4, the system recovers when applied at 3 s, and does not recover when applied at 3.1 s. Once again, these results are consistent with the practical use of TEF.

3) Conclusions: From the previous analysis, one can conclude that shunt compensation and load shedding have a positive effect on system recovery, as expected and demonstrated below for a real system; however, the problem is to determine how much and how fast. Observe that one could define "optimal" values of compensation and load shedding, i.e., the "minimum" compensation and/or load shedding that allows to recover the system within "reasonable" application times. The answer would depend on how much compensation and load to be shed is available, as well as the response times of the switching devices controlling these system elements. Furthermore, shunt and load location should also be considered, as it is well known that physical location of these elements has an effect on the stability of the system. Control limits, such as generator AVR limits, should also be factored into the analysis, as these have a significant negative effect on the stability regions, increasing the compensation and load shedding levels and reducing the associated application times required to recover the system.

Notice that the TEF is mainly used in this simple example to illustrate the relative effect of compensation and load shedding on system stability. The example presented here clearly shows that TEFs can mainly be used in practice as a screening tool to classify the relative severity of contingencies or the goodness of recovery strategies. The authors are currently researching reliable criteria and techniques based on TEF analyses that could be used in realistic systems to determine "optimal" compensation and load shedding levels as well as their corresponding application times.

III. Voltage Collapse in the CIS

A real voltage collapse problem on The Chilean Interconnected System (CIS) occurred in May 1, 1997, it is used here to demonstrate the issues discussed above regarding timing and sizing of shunt compensation and load shedding as recovery strategies from collapse. This system with about 500 buses, covers an area of 2000 km in length, supplying a load over 3000 MW. The annual load increase rate, during the last five years, has been approximately 8% on average [15].

The basic structure of this system is illustrated in Fig. 8 through a simplified 17-bus system. The major load is located in Santiago, Chile's capital, in a ring formed by three buses: Polpaico, Cerro Navia and Alto Jahuel. The latter is the main bus receiving energy from power sources located in southern Chile. In this representation there are 7 main power sources; these include five hydro generating plants in the southern and central areas (Colbun-Pehuenche, Pangue, El Toro-Antuco, Isla-Cipreses and Rapel), and two thermal generating units in the central and northern areas (Ventanas and Guacolda).

This power system is represented by a set of differential-algebraic (DAE) equations somewhat similar to (1) [28], [29], i.e.,

$$\dot{x} = f(x, y, z, p)$$
$$0 = g(x, y, z, p)$$

where x is the vector of dynamical variables of the network, y is the vector of algebraic variables, z is the vector representing control variables, p is a vector representing the fixed variables and parameters of the system, f is a set of nonlinear differential equations, and g is a set of nonlinear algebraic equations.

Loads are represented by an exponential model [30], and generators by a one-axis model [29]. The values used for the generator parameters are estimated by using both international available data and information on the actual generators. Automatic Voltage Regulators (AVR) are modeled by a first-order transfer function connected in series with a voltage limiter [7], which has maximum and minimum transient voltage limits and maximum steady-state limits, as depicted in Fig. 9. The voltage limiter is activated once the excitation exceeds its transient limit value for more than τ seconds; in the simulations this limit is chosen as 10 seconds. This excitation voltage limiter or maximum excitation

limiter (MXL) plays a key role in the voltage collapse of this system as explained in the following sections. The tap mechanism in the transformers with On Load Tap Changers (OLTC) is simulated through a special function that uses a tolerance ε and a dead-time of τ_1 seconds. Once the OLTC is activated, a tap change is produced every τ_2 seconds, as long as the secondary voltage is outside the tolerance ε.

Time simulations are carried out using MATLAB, where a time scaling technique is used in order to increase the efficiency of the algorithm; thus, one second of simulation stands for 1 minute in the real event.

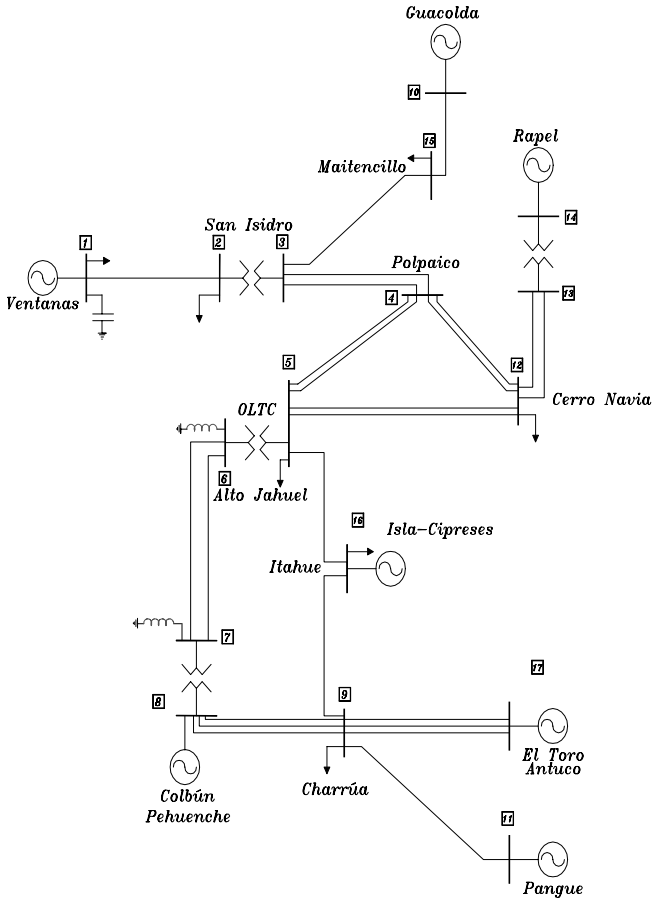

Fig. 8. The Chilean Interconnected System (CIS).

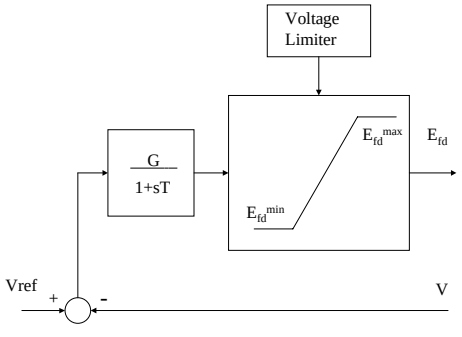

Fig. 9. AVR with dynamic limits.

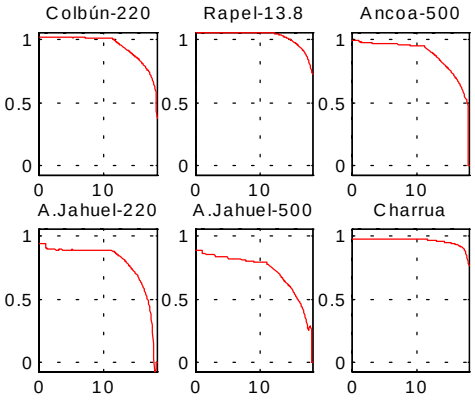

Fig. 10. Evolution of p.u. bus voltages. Time scale in minutes.

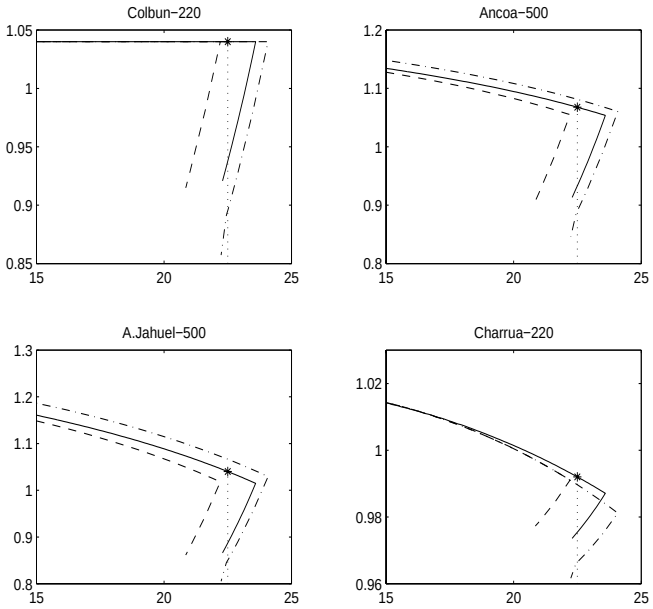

Fig. 11. Voltage profiles in p.u with respect to total loading conditions in MVA. Continuous lines correspond to the base system (the * marks the current loading conditions); dashed lines correspond to the faulted system; dash-dotted lines correspond to the faulted system with 200 MVar capacitive support added at the A.Jahuel bus.

A. *Voltage Collapse Scenario*

The voltage collapse scenario studied in this paper is the outage of the 154 kV line from Itahue to Alto Jahuel, which actually happen in the CIS in May 1997 at 23:23 hrs. [15]. After this fault, the system was recovered in approximately 30 minutes. During the incident, approximately 80% of the system load was lost.

In order to illustrate this voltage collapse, the evolution of the voltage at the main system's buses is shown in Fig. 10. These simulations clearly depict the typical evolution of voltage collapse observed in other systems [1], [2], [11]-[14], i.e., a slow and steady decreasing value of voltage, followed by a rapid decay. Observe that the Alto Jahuel buses decay faster than the Charrua bus, as the latter bus is more distant in terms of electrical impedance to the "critical" area than the other buses depicted in this figure.

The longitudinal structure of the CIS is similar to other networks where voltage collapse incidents have been experienced in the last

few years [7], [10], [12], [13]. In reference [7], the author analyzes in detail a voltage collapse in a 4-bus network with a structure similar to the CIS; this system has a generating center that is located far from the demand, with an additional generating unit in the middle of the transmission line connecting both ends. A similar structure can be observed in the test system used in [10] and in the real systems of [12] and [13]. All these references show that a longitudinal system with a generating unit located near the middle of the network is prone to voltage instabilities; the voltage collapse occurs when the generating unit in the middle of the system reaches excitation control limits.

The main cause for the steep descent rate of the voltage profiles in the CIS is the overexcitation limits in generating units, mainly Colbun-Pehuenche, which is the main cause of the voltage collapse [15]. This is confirmed by steady state analyses, which yield the voltage profiles depicted in Fig. 11. Observe that the system collapses due to a maximum Q-limit at the Colbun-Pehuenche generating bus when the Itahue-A.Jahuel line is removed (faulted system), as there is no power flow solution for this system at the given loading conditions. When a 200 MVar static bank of capacitors currently available at the A.Jahuel bus in Santiago is added to the faulted system or when the load is shed, the equilibrium point is recovered, as demonstrated by the voltage profiles in Fig. 11. Thus, based on the theoretical analysis presented in Section II, the problem is then to determine when to apply shunt capacitive support or shed load to avoid the voltage collapse triggered by the overexcitation limits of the Colbun generators; this problem is thoroughly analyzed in the next two sections.

B. Shunt Compensation

We select three different time instants to simulate the connection of the 200 MVar bank of capacitor at the A.Jahuel bus. In the first case, this action is taken just after the first generator, Colbun, reaches overexcitation limits, i.e., at minute 12 of the simulation. In the second case, this action is simulated just before reaching the overexcitation limits at Colbun, i.e., at minute 11. Finally, the third case is simulated after the tripping of the line, approximately at 1.2 minutes (12 seconds after the tripping of the line). For each case we record the voltage evolution in the main buses of the system.

The time evolution of the voltages is presented in Fig. 12 for the case when the var injection occurs after the overexcitation limits in Colbun (minute 12). Observe that the bus A. Jahuel-220 clearly shows an increase in voltage magnitude after the bank of capacitors is connected; this voltage rise is also observed in the Rapel-13.8 and A. Jahuel-500 buses. The increase lasts for about 3 minutes, after which the bus voltages collapse in all buses. In the Charrua bus, the rate of decay is smaller due to the longer electrical distance to the Colbun bus area.

Hence, this test clearly shows that the effect of reactive power injection after the overexcitation limits of the generators is not enough to stop the voltage collapse. In the authors' view, this is the main reason for the unsuccessful attempts of var compensation that was experienced in the real incident. However, this is not necessary always the case, as it can be seen on the simulations of the test system in Section II.

When the MVar injection is applied just before reaching overexcitation limits at Colbun (minute 11), all voltages recover, after a momentary dip, as depicted in Fig. 13. In this case, the reactive power injection produces a notorious improvement on all system voltages, successfully recovering the system by avoiding reaching limits on the generators' field voltages.

The time evolution of the voltages when the static bank of capacitors is applied immediately after the line outage (minute 1.2.) is shown in Fig. 14. In this case, the application of reactive compensation improves significantly the voltage evolution of the power grid; in fact, all bus voltages reach an equilibrium point after the first five minutes.

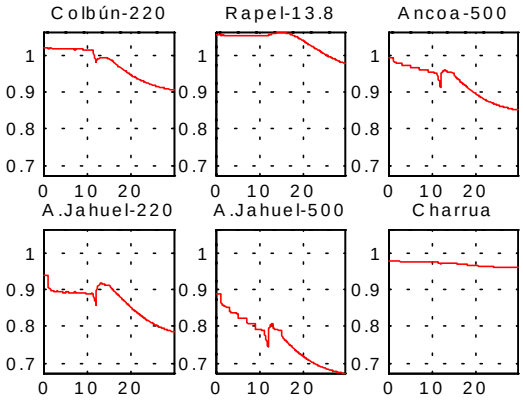

Fig. 12. Post-limits var injection. Time scale in minutes.

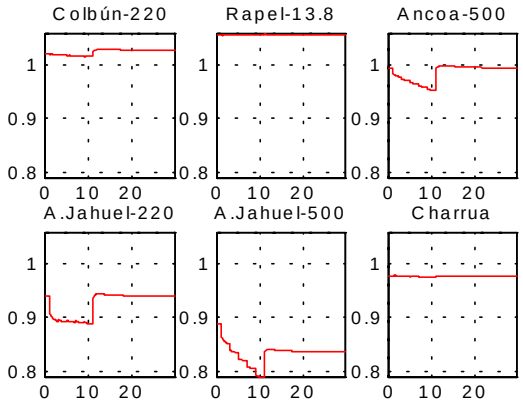

Fig. 13. Pre-limits var injection. Time scale in minutes.

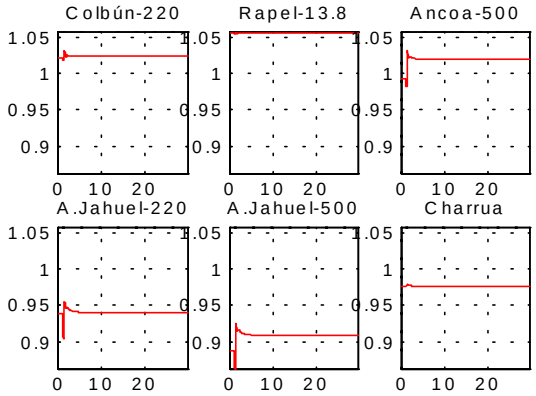

Fig. 14. Var injection immediately after line fault. Time scale in minutes.

The results clearly indicate that the faster the reactive compensation is applied, the faster the system recovers; if it is too slow, the system might collapse, which is what was expected from the theoretical analysis presented in Section II. Thus, similar to the critical clearing time concept in angular stability, there exists an

equivalent "critical compensation time" which corresponds to the maximum time available to take control actions before the systems exits the stability region. A similar concept for time constants of OLTC transformers is developed in [31].

C. Load Shedding

In these tests we assume that load shedding is performed in steps of equal load blocks. Thus, in order to avoid voltage collapse, each load block is disconnected from a set of buses as long as transient excitation voltage limits in generators are violated. Then we investigate the effect of changing this time interval at which the steps of load are shed; the first interval is selected to be 90 s, i.e., blocks of load are disconnected from the network each 90 s, and the second interval is chosen to be 180 s.

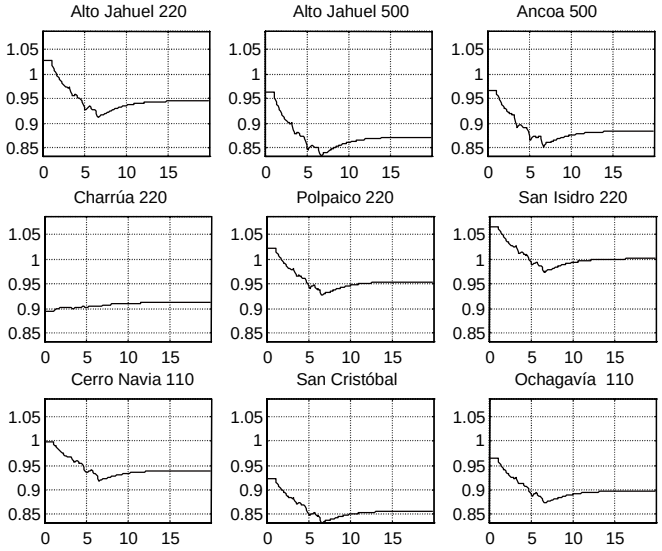

Fig. 15. Evolution of p.u. voltages for 90 s load shedding intervals. Time scale in minutes.

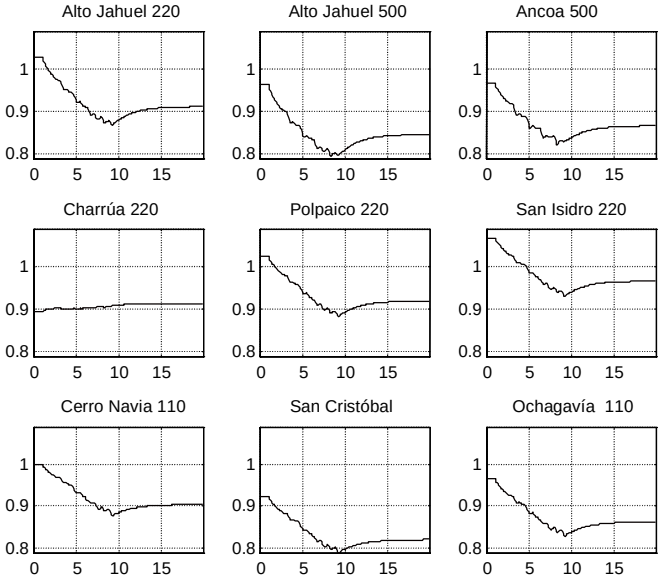

Fig. 16. Evolution of p.u. voltages for 180 s load shedding intervals. Time scale in minutes.

The other relevant parameters involved in this control action are the identification of the set of load buses eligible for load shedding, the time to start the load curtailment and the amount of load to be disconnected from the network. Thus, the closest load bus to the generators reaching their maximum excitation control are chosen to be shed; then, a set of load buses with the least electrical distance to each generator are identified. The load shedding starts when a generator reaches it maximum transient excitation limit. Blocks of 10% are disconnected from each load bus as long as the excitation voltage is over the corresponding transient limit value.

In order to illustrate the effects of this control action on the system, two buses belonging to the ring of buses of the load center are added to the voltage profile graphs; these are San Cristobal and Ochagavía.

Figure 15 illustrates the effect of performing load shedding each 90 s. Observe that bus voltages drop during the first 5 minutes after the perturbation, after about 6 minutes a recovery process is observed, and after 15 minutes the voltages stabilize. The total load disconnected from the network is 101 MW/55 MVar.

In Fig. 16, the evolution of bus voltages for load shedding intervals of 180 s is presented. Although the voltage drop lasts for approximately 9 minutes (two more minutes than in the previous case), the voltages recover after 15 minutes. Although the final voltage levels are lower than when using the shorter interval, the total load disconnected from the network of 70 MW/36 MVar is significantly smaller in this case (about 70% of the previous load shed). Thus, when a larger interval is used for the control action, we obtain an economy in the load curtailment.

Observe that load shedding has certain "inertia" on the system voltage profile, i.e., it takes a few minutes to observe its effect on the excitation control of the generators. This explains the poor voltage profiles when the time load shedding interval is increased. The system behavior suggests that there is an optimal amount of load and time interval for load shedding, as expected from the theoretical analysis presented in Section II.

IV. Conclusions

This paper presents a detailed study of the time dependence of control actions to avoid voltage collapse in real systems. A voltage collapse that took place in the actual Chilean system is studied, demonstrating that overexcitation limits in key generating units is the leading factor for the collapse problem in this particular system.

The analyses and results presented here show that the types and timing of control actions taken to avoid voltage collapse are critical for the success of emergency controls. In particular, the size and timing of var compensation and load shedding determine whether these control actions succeed in avoiding collapse. This is of special importance for load shedding, as one could develop strategies to minimize load interruption. The authors are currently working on a practical mechanism to determine critical control times and levels to avoid collapse in realistic systems.

V. Acknowledgment

This paper has been partially supported by a grant Fondap Matematicas Aplicadas and the Facultad de Ciencias Fisicas y Matematicas de la Universidad de Chile, and by a grant from NSERC, Canada.

REFERENCES

[1] "Survey of the Voltage Collapse Phenomenon," Technical Report, North American Electric Reliability Council, 1990.

[2] L. H. Fink, Ed., *Bulk Power System Voltage Phenomena II—Voltage Stability Security and Control*, ECC/NSF Workshop, Davos, Switzerland, August 1994.

[3] H. K. Clark, New Challenge: Voltage Stability, *IEEE Power Engineering Review*, pp. 33-37, April 1990.

[4] L. H. Fink, Concerning Voltage Control, pp. 3-5 in [2].

[5] L. Vargas and V.H. Quintana, "Dynamical Analysis of Voltage Collapse in Longitudinal Systems," Electrical Power & Energy Systems, Vol. 16, No. 4, pp. 221-228, 1994.

[6] L. Vargas, "Improving Voltage Stability in Power Systems," *Proceedings of the Fourth Seminar on System Identification, Parameter Estimation and Adaptive Control*, Santiago, Chile, pp. 289-295, 1995.

[7] T. Van Cutsem, "Voltage Collapse Mechanism-A case Study," *Bulk Power System Voltage Phenomena II-Voltage Stability and Security*, pp. 85-101, August 1991.

[8] P. Rousseaux and T. Van Cutsem, "Fast Small-Disturbance Analysis of Long-Term Voltage Stability," *12th Power Systems Computation Conference*, Dresden, pp. 295-302, August 19-23, 1996.

[9] T. Van Cutsem and R. Mailhot, "Validation of a Fast Voltage Stability Analysis Method on the Hydro-Quebec System," *IEEE Transactions on Power Systems*, Vol. 12, No. 1, pp. 282-292, Feb. 1997.

[10] G.K. Morrison, B. Gao, and P. Kundur, "Voltage Stability Analysis Using Static and Dynamic Approaches," *IEEE Transactions on Power Systems*, Vol. 8, No. 3, pp. 1159-1171, August 1993.

[11] IEEE Working Group on Voltage Stability, "Voltage Stability of Power Systems: Concepts, Analytical Tools, and Industry Experience," 90TH0358-2-PWR, IEEE Tutorial Course, 1990.

[12] Y. Hain and I. Schweitzer, "Analysis of the Power Blackout of June 8, 1995 in the Israel Electric Corporation," *IEEE Transactions on Power Systems*, Vol. 12, No. 4, pp. 1752, pp. 1752-1757, November 1997.

[13] R. Hirvonen and L. Pottonen, "Low Voltages after a Disturbance in the Finnish 400 kV Network," pp. 231-239 in [2].

[14] R. J. O'Keefe, R. P. Schultz, and N. B. Bhatt, "Improved Representation of Generator and Load Dynamics in the Study of Voltage Limited Power System Operations," *IEEE Transactions on Power Systems*, Vol. 12, No. 1, pp. 235-239, Feb. 1997.

[15] T. J. Overbye, "Computation of a Practical Method to Restore Power Flow Solvability," *IEEE Tans. Power Systems*, Vol. 10, No. 1, pp. 280-287.

[16] L. Vargas, V. H. Quintana and R. Miranda, "Voltage Collapse Scenario in the Chilean Interconnected System," to appear in *IEEE Transactions on Power Systems, PE-214-PWRS-0-12-1998*.

[17] E. De Tuglie, M. La Scala, and P. Scarpellini, "Real-time Preventive Actions for the Enhancement of Voltage-degraded Trajectories," to appear in *IEEE Transactions on Power Systems*, PE-020-PWRS-0-06-1998.

[18] C. A. Cañizares, "Calculating Optimal System Parameters to Maximize the Distance to Saddle-node Bifurcations," *IEEE Trans. Circuits and Systems-I*, Vol. 45, No. 3, pp. 225-237, March 1998.

[19] M. A. Pai, *Energy Function Analysis for Power System Stability*, Kluwer Academic, 1989.

[20] T. J. Overbye and C. L. DeMarco, "Voltage Security Enhancement Using Energy Based Sensitivities," *IEEE Trans. Power Systems*, Vol. 6, No. 3, pp. 1196-1202, August 1991.

[21] M. Vidyasagar, *Nonlinear System Analysis*, Second Edition, Prentice Hall, 1993.

[22] C. L. DeMarco and C. A. Cañizares, "A Vector Energy Function Approach for Security Analysis of AC/DC Systems," *IEEE Trans. Power Systems*, Vol. 7, No. 3, August 1992, pp. 1001-1011.

[23] P. Kundur, G.K. Morison, and L. Wang, "Techniques For On-line Transient Stability Assessment and Control," *Proc. IEEE/PES Winter Meeting*, paper 0-7803-5938-0/00, Singapore, January 2000.

[24] C. A. Cañizares and F. L. Alvarado, "Point of Collapse and Continuation Methods for Large AC/DC Systems," *IEEE Trans. Power Systems*, Vol. 8, No. 1, pp. 1-8, February 1993,

[25] I. Dobson and L. Lu, "Voltage Collapse Precipitated by Inmediate Change in Stability when Generator Reactive power Limits are Encountered," *IEEE Trans. Circuits and Systems-I*, Vol. 39, No. 9, pp. 762-766, Sept. 1992.

[26] H. D. Chiang and F. F. Wu, "Stability of Nonlinear Systems Described by a Second-Order Vector Differential Equation," *IEEE Trans. Circuits and Systems*, Vol. 35, No. 6, pp. 703-711,June 1988.

[27] C. A. Cañizares and S. Hranilovic, "Transcritical and Hopf Bifurcations in AC/DC Systems," pp. 105-114 in [2].

[28] P. M. Anderson and A. A. Fouad, *Power System Control and Stability*, Iowa State University Press, Ames, Iowa, USA, 1977.

[29] J. Arrillaga, C. P. Arnold and B. J. Harker, *Computer Modeling of Electrical Power Systems*, John Wiley & Sons, 1983.

[30] IEEE Task force on Load Representation for Dynamic Performance, "Load Representation for Dynamic Performance Analysis," *IEEE Transactions on Power Systems*, Vol. 8, No. 2, pp. 213-221, May 1993.

[31] D. H. Popovic, D. Hill, and I. A. Hiskens, "Oscillatory Behavior of Power Supply Systems with a Single Dynamic Load," *12th Power Systems Computation Conference*, Dresden, pp. 888-894, August 19-23, 1996.

Luis S. Vargas (M) received the Electrical Engineer diploma (1985) and M.Sc. degree (1987) from the Universidad de Chile, Santiago, Chile. He obtained his Ph.D. degree in Electrical Engineering (1993) from the University of Waterloo, Ontario, Canada. Dr. Vargas is currently a professor at the Universidad de Chile. He has been involved in applied projects for companies in Chile, and his main research activities are in the areas of voltage stability, security and deregulation of the electric utilities.

Claudio A. Cañizares (S 86, M 91) received the Electrical Engineer diploma (1984) from the Escuela Politécnica Nacional (EPN), Quito-Ecuador, where he held different positions from 1983 to 1993. His M.Sc. (1988) and Ph.D. (1991) degrees in Electrical Engineering are from the University of Wisconsin-Madison. Dr. Cañizares is currently an Associate Professor at the University of Waterloo and his research activities mostly concentrate on the study of computational, modeling, and stability issues in ac/dc/FACTS power systems.